

Numerical and experimental analyses for RO desalination systems using a static pressure head

Osamu Miyatake*, Kotaro Tagawa

*Department of Chemical Engineering, Graduate School of Engineering, Kyushu University, Fukuoka 812-8581, Japan
Tel. & fax: +81 (92) 642-3514; email: miyatake@chem-eng.kyushu-u.ac.jp*

Received 25 July 2000; accepted 8 August 2000

Abstract

Numerical and experimental analyses were performed for the RO desalination system using a static pressure head, during which two cases of the system channel configuration were considered. One case was where only one side of the annular channel was laminated with the RO membrane, and the other was where both sides of the annular channel were laminated with the RO membrane. In both cases numerical results were obtained for the effects of the width and the axial length of the channel, the submerged depth, the pure water permeability and the solute permeability of membrane, and the physical properties of seawater or brackish water on the axial variation of velocity, concentration, and pressure in laminar natural convection flow, caused by the concentration difference in the moderately narrow channel. The effect of these parameters on the axial variation of the flow rate of transmitted fresh water was also examined. From the numerical results the dimensionless expressions were formulated to predict the flow rate of transmitted fresh water from the parameters. The field experiments on the desalination system of seawater using a static pressure head due to the depth of the sea in the former case were carried out in the East China Sea and the Sea of Japan. Experimental results of the flow rate of transmitted fresh water permeated through the membrane were found to be in good agreement with the expression, and the applicability and the usefulness of the expression were confirmed.

Keywords: Membrane separation; Reverse osmosis; Desalination; Static pressure head; Numerical analysis; Field experiment

1. Introduction

The reverse osmosis (RO) technique with using static pressure due to the depth of the sea or a dead pit filled with brackish water has been

considered for the development of a desalination device to be used to obtain fresh water from seawater or brackish water without applying any pressure by a pump as in the conventional RO seawater desalination device based on the land. This method of the RO seawater desalination system is energy saving because the specific

*Corresponding author.

Presented at the conference on Desalination Strategies in South Mediterranean Countries, Cooperation between Mediterranean Countries of Europe and the Southern Rim of the Mediterranean, sponsored by the European Desalination Society and Ecole Nationale d'Ingenieurs de Tunis, September 11–13, 2000, Jerba, Tunisia.

power consumption needed to pump up fresh water to the water surface is considerably lower in comparison with those needed by the land-based RO seawater desalination system.

In previous studies, the idea and the energy efficiency of the RO desalination system using a static pressure head, which feeds seawater and brackish water into the RO module by forced convection by the pump, were reported [1–5]. However, these reports were based on the predetermined performance of the RO module.

In the present study, a new idea of developing a desalination system in which the RO membrane with both ends open is installed vertically and submerged in seawater or brackish water has been considered. The concentrated seawater or brackish water flows through the channel in the RO module by natural convection caused by the concentration difference.

The two cases of channel configuration of the system considered for the present study are shown in Fig. 1. In one case (a) where only one side of the channel is laminated with the RO membrane, a lot of tube type membrane is put into a cylindrical vessel and cylindrical rods are

placed inside the tubes in such a way so that the narrow annular channels between the tube and the rod are formed. In the other case (b) where both sides of the channel are laminated with the RO membrane, narrow annular channels are formed in a cylindrical vessel and the membrane is laminated on both sides of the channel.

Firstly, a numerical analysis was performed for the RO desalination system of seawater or brackish water for the case where only one side of the channel was laminated with the RO membrane in the general case with the water and solute permeation through the membrane. Secondly, the field experiments on the RO seawater desalination system using static pressure due to the depth of the sea were carried out in the case of that channel. Furthermore, a numerical analysis was performed for the RO seawater desalination system in the case where both sides of the channel were laminated with the RO membrane, disregarding the solute permeation through the membrane.

The purpose of this paper is to clarify the effects of various factors on several characteristics and transmitted fresh water of the

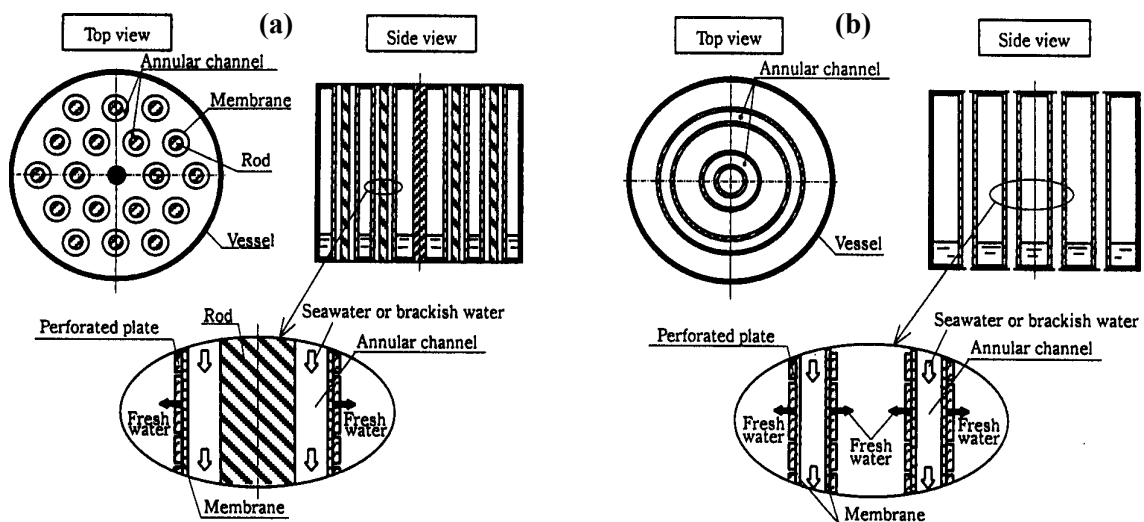


Fig. 1. Schematic description of the RO module. (a) Case where only one side of channel is laminated with the RO membrane. (b) Case where both sides of the channel are laminated with the RO membrane.

desalination system, and to present the information for the optimum design of the system from numerical and experimental results.

2. Numerical analysis for the RO desalination system in the case where only one side of the channel is laminated with the RO membrane

2.1. Fundamental equations and analytical procedure

The moderately narrow annular channel formed between the tube-type membrane and a cylindrical rod can be approximated to a channel formed by two vertical parallel plates. The analytical system and coordinates are shown in Fig. 2. The channel consisted of two parallel plates, having a finite axial length l and separated by a distance b , vertically placed in seawater and brackish water of depth δ , and concentration c_0 . One of the plates is the RO membrane, which

permeates water and some solute through the membrane, while the other is the non-permeated plate.

The fundamental equations (continuity, motion and mass diffusion), the boundary conditions, and the equations related to these equations and boundary conditions take the following form.

$$\frac{\partial U}{\partial X} + \frac{\partial V}{\partial Y} = 0 \tag{1}$$

$$U \frac{\partial U}{\partial X} + V \frac{\partial U}{\partial Y} = -\frac{dP}{dX} + \frac{\partial^2 U}{\partial Y^2} + (C-1) \tag{2}$$

$$U \frac{\partial C}{\partial X} + V \frac{\partial C}{\partial Y} = \frac{1}{Sc} \frac{\partial^2 C}{\partial Y^2} \tag{3}$$

$$X=0, \quad 0 < Y < 1; \quad U = (Q)_{X=0}, \quad V=0, \quad C=1 \tag{4}$$

$$\left. \begin{aligned} X \geq 0, \quad Y=0; \quad U=0, \quad V=V_w \\ \Psi(C_w - C^*) + C_w V_w = (1/Sc)(\partial C / \partial Y)_w \end{aligned} \right\} \tag{5}$$

$$Y=1, \quad X \geq 0; \quad U=0, \quad V=0, \quad (\partial C / \partial Y) = 0 \tag{6}$$

$$X=0; \quad P = -(Q)_{X=0}^2 / 2 \tag{7}$$

$$X=L; \quad P=0 \tag{8}$$

$$\begin{aligned} V_w = -\Phi \left(1 - \frac{C_w - C^*}{\Delta} \right) \left(\frac{\rho^o}{\rho_w} \right) \\ - \Psi(C_w - C^*) \left(\frac{c_0}{\rho_w} \right) \end{aligned} \tag{9}$$

$$C^* = \frac{\Psi(C_w - C^*)}{(-V_w)(\rho_w / \rho^*)} \tag{10}$$

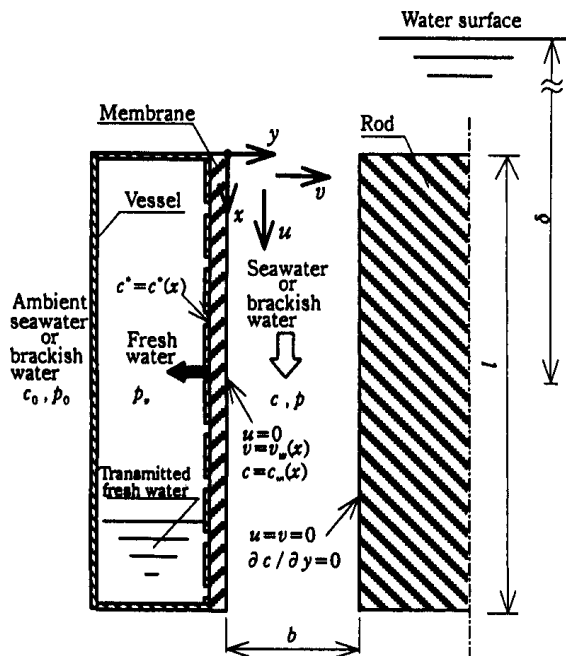


Fig. 2. Analytical system and coordinates.

$$Q = \int_0^1 U dY = (Q)_{X=0} + \int_0^X V_w dX \quad (11)$$

$$C_m Q = \int_0^1 C U dY = C_0 (Q)_{X=0} - \int_0^X \Psi (C_w - C^*) dX \quad (12)$$

$$\overline{C^*} = \frac{\int_0^X \Psi (C_w - C^*) dX}{\int_0^X [\Psi (C_w - C^*) / C^*] dX} \quad (13)$$

$$Q^\circ = \int_0^L \Phi [1 - (C_w - C^*) / \Delta] dX \quad (14)$$

where

$$\left. \begin{aligned} U &= bu / (v\Gamma), \quad V = bv / v, \quad C = c/c_0 \\ P &= b^2(p-p_0) / (\rho v^2 \Gamma^2), \quad X = x / (b\Gamma), \\ Y &= y/b, \quad L = l / (b\Gamma), \quad \Delta = \rho g \delta / \pi_0, \\ \Phi &= \rho g \delta b \phi / v, \quad \Psi = b \psi / v, \quad Sc = v/D, \\ Q &= bu_m / (v\Gamma), \quad Q^\circ = q^\circ / (v\Gamma), \\ C^* &= c^* / c_0, \quad \overline{C^*} = \overline{c^*} / c_0, \quad \Gamma = b^3 g c_0 \gamma / v^2 \end{aligned} \right\} \quad (15)$$

The dimensionless induced flow rate at the channel inlet $(Q)_{X=0}$ and the dimensionless axial length of the channel L are not independent of each other, but L can be determined if $(Q)_{X=0}$ is given. In addition, the case without the solute

permeation through the membrane corresponds to the dimensionless solute permeability $\Psi=0$, and the case with the solute permeation corresponds to $\Psi \neq 0$.

The numerical analysis is carried out by writing the fundamental equations Eqs. (1)–(3) in finite difference form and then solving them with the boundary conditions Eqs. (4)–(8) using a forward marching, implicit method with iteration at each level of X . Furthermore, the values of U , V , C , C^* and P , which satisfy with Eqs. (9)–(12), are evaluated at each level. Finally, the dimensionless mean concentration of transmitted fresh water $\overline{C^*}$ and the dimensionless flow rate of transmitted pure water Q° are calculated from Eqs. (13) and (14).

2.2. Numerical results

Typical results of the axial variation of the dimensionless velocity and concentration profiles are shown in Fig. 3. The profile of U in the figure gradually takes a parabolic profile from a uniform profile. As seawater and brackish water flow through the channel in the downward direction, natural convection in the neighborhood of the membrane wall is increased with the rise in concentration of seawater or brackish water. Therefore, the velocity profile U moves slightly toward the membrane wall. When the dimensionless solute permeability Ψ is high, the amount of transmitted pure water increases (see Fig. 5). Consequently, U decreases and C increases. When the dimensionless induced flow rate at the channel inlet $(Q)_{X=0}$ is large, the dimensionless length of the channel L corresponded to $(Q)_{X=0}$ is long. Consequently, C increases since the amount of transmitted pure water increases.

Typical results of the axial variation of the dimensionless horizontal velocity at the membrane wall V_w , the dimensionless concentration of seawater or brackish water at the membrane wall C_w , and the dimensionless concentration of transmitted fresh water C^* are shown in Fig. 4.

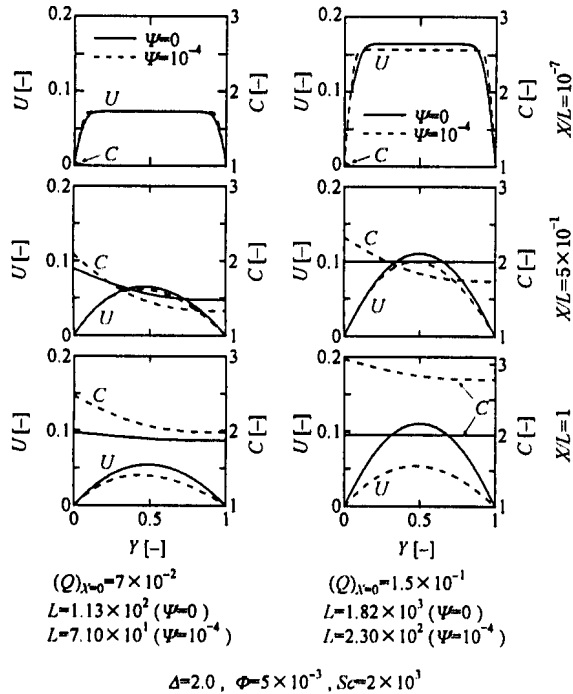


Fig. 3. Axial variation of dimensionless velocity and concentration profiles in channel.

The marks of open circles in the figure refer to conditions at the channel outlet. When Ψ is high, $-V_w$, C_w and C^* increase, but $C_w - C^*$ decreases. These phenomena are the consequence of a series of occurrences. First, C^* increases with the solute permeation. Then, since the contribution of fresh water permeation [the first term of the right side of Eq. (9)] is large in comparison with the contribution of solute permeation [the second term of the right side of Eq. (9)], $-V_w$ increases consequently. Furthermore, the amount of solute carried to the membrane wall gains with the increase of $-V_w$, C_w and C^* increase rapidly along X direction. However, C^* increases at a greater rate in comparison with the rise of C_w , causing $C_w - C^*$ to decrease.

Typical results of the dimensionless flow rate of transmitted pure water Q° are shown in Fig. 5. When Ψ is high, Q° increases from the relation

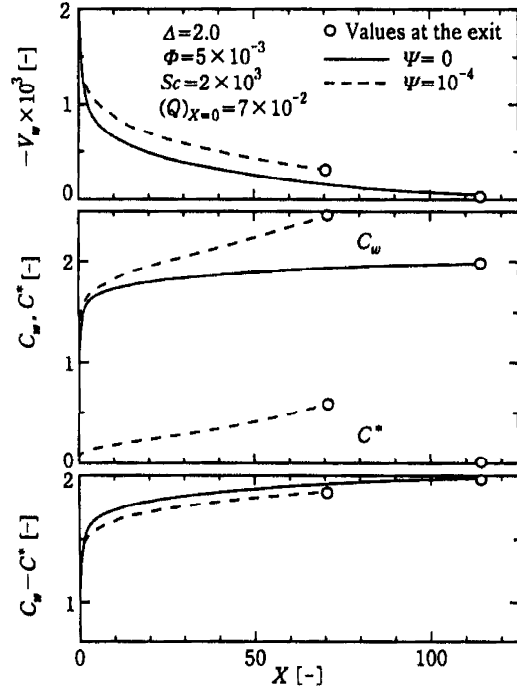


Fig. 4. Axial variation of dimensionless horizontal velocity and solute concentration at the membrane wall in channel, and dimensionless solute concentration of transmitted fresh water.

of Eq. (14) as shown in Fig. 4, since the concentration difference between seawater or brackish water and transmitted fresh water at both sides of the membrane decreases. When Δ is deep, Q° increases since the dimensionless driving pressure difference for the water permeation $[=\Delta - C_w]$ increases. When L is long and Φ is high, Q° increases consequentially. The effect of Sc on Q° is not distinguishable in Fig. 5 because the abscissa is Sc/L . When Sc is large, Q° decreases with the concentration polarization.

In the case of disregarding the solute permeation, that is, in the case of $\Psi = 0$, as L is longer (Sc/L is smaller), Q° approaches the maximum value (Q°_{max}) given by the following equation derived theoretically.

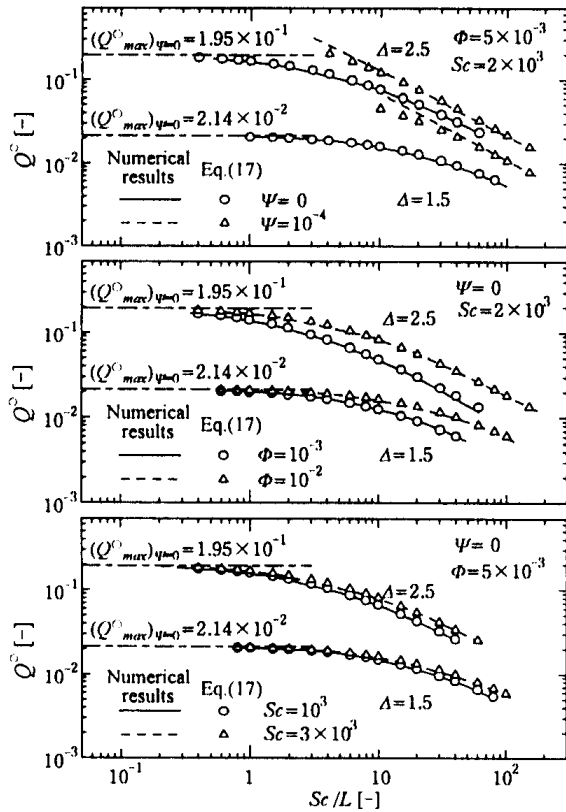


Fig. 5. Dimensionless flow rate of transmitted pure water in the case where only one side of the channel is laminated with the RO membrane.

$$(Q^o_{max})_{\Psi=0} = (1/12)(1.012 + 0.012\Delta)(\Delta - 1)^2 \quad (16)$$

It is important that the expression of Q^o is formulated from the numerical results in order to make an optimum design of the desalination system. Q^o is obtained from the numerical results as

$$\left. \begin{aligned} Q^o &= \varepsilon(Q^o)_{\Psi=0}; \quad \varepsilon = \exp \left[\frac{0.65\Psi^{0.45} Sc^{0.60}}{(\Delta - 1)^{0.75} (Sc/L)^{0.20}} \right] \\ (Q^o)_{\Psi=0} &= (Q^o_{max})_{\Psi=0} \left[1 + \alpha(Q^o_{max})_{\Psi=0} (Sc/L) \right]^{-0.78} \\ \alpha &= \frac{2.20}{[\Phi(1 - 1/\Delta)Sc]} + \frac{2.55}{\Delta^{1.20}} \end{aligned} \right\} \quad (17)$$

where ε is the ratio of (Q^o) , which increases with the effect of the solute permeation, to $(Q^o)_{\Psi=0}$.

The calculated values from Eq. (17), shown by the marks in the figure, are in good agreement with numerical results. From these results, the prediction of numerical results of Q^o from L , Δ , Φ , Ψ , and Sc is possible.

3. Field experiment for the RO desalination system in the case where only one side of the channel is laminated with the RO membrane

The experimental apparatus used in the field experiment is shown in Fig. 6. The apparatus consists of a vertical stainless steel pressure vessel with a diameter of 48.8 mm, a length of 1054 mm, and a perforated stainless-steel tube with the tubular membrane attached to its inner surface installed vertically inside the vessel. The tubular membrane has a length of 1034 mm while its inner diameter is 11.5 mm. In addition, stainless-steel rods with four different diameters of 5.0, 6.0, 7.0 and 8.0 mm were installed at the center of the tube. The moderately narrow annular channel is formed between a tube and a rod. The field experiments were conducted in the East China Sea and the Sea of Japan. The experimental apparatus descended at a velocity of 1 m/s to a depth of 600 m and 520 m from the surface of the sea, and then either ascended immediately or was kept at that position for a predetermined time, depending on the objective of the experiment, and ascended at a velocity of 1 m/s up to the surface of the sea. Then the concentration and the amount of transmitted fresh water were measured.

The comparison of Eq. (17) with experimental results for the flow rate of transmitted pure water per unit width of the channel q^o is shown in Fig. 7. The lines are the values of q^o from Eq. (17). The marks are those from the experimental results. Also, the value of q^o from Eq. (17) when solute permeation through the

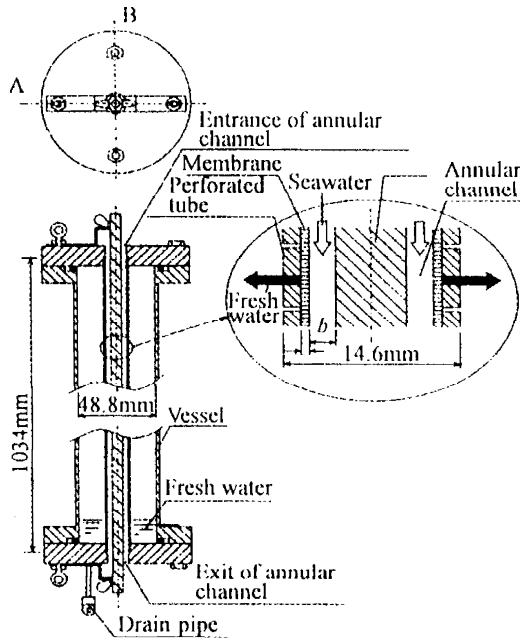


Fig. 6. Schematics of the experimental apparatus.

membrane is disregarded are also shown in the figure. Regardless of the solute permeation, q° exhibits an increase with decreasing width of the channel up to a maximum at a width of about 1–2 mm, followed by a rapid decrease; thus the existence of the optimum width of the channel is understood. In the case of the solute permeation, the concentration difference between both sides of the membrane decreases with the rise of concentration of transmitted fresh water. Since the driving pressure force for the water permeation increases by that effect in comparison with that in the case of disregarding solute permeation, q° increases. It is found that Eq. (17) shows good agreement with the experimental results and the applicability of Eq. (17) is thus confirmed.

4. Numerical analysis for the RO desalination system in the case where both sides of the channel are laminated with the RO membrane

This numerical analysis for the case where both sides of the channel are laminated with the RO membrane, for the case where only one side of the channel is laminated with the RO membrane, except that there is only the water permeation through the membrane on both sides of the channel, and the case with disregarding the solute permeation. In this analysis the dimensionless flow rate of transmitted pure water is expressed by the following equation:

$$Q^\circ = 2 \int_0^L \Phi (1 - C_w / \Delta) dX \quad (18)$$

This analysis was carried out by the same procedure as described in Section 2.

Typical results of the dimensionless flow rate of transmitted pure water Q° are shown in Fig. 8. When L is long, Δ is deep and Φ is high, Q° increases consequentially. Also, Q° approaches the maximum value (Q°_{max}) expressed by Eq. (16) for the case where only one side of the channel is laminated with the RO membrane.

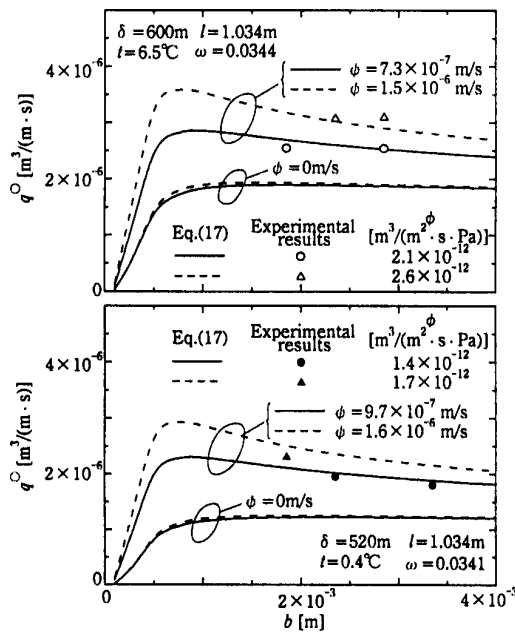


Fig. 7. Comparison of Eq. (17) with experimental results for the flow rate of transmitted pure water per unit width of the channel.

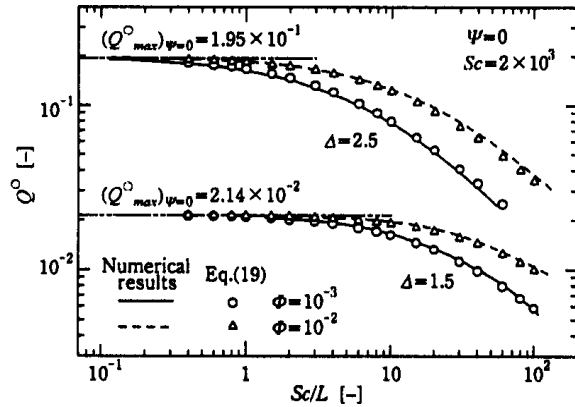


Fig. 8. Dimensionless flow rate of transmitted pure water for the case where both sides of the channel are laminated with the RO membrane.

From numerical results in this analysis, the expression of Q^o is obtained as

$$Q^o = \left(Q^o_{max} \right)_{\Psi=0} \left[1 + \alpha \left(Q^o_{max} \right)_{\Psi=0} (Sc/L)^{-0.78} \right] \quad (19)$$

$$\alpha = \frac{0.91}{\Phi (1 - 1/\Delta) Sc} + \frac{1.05}{\Delta^{1.20}}$$

The calculated values from Eq. (19), shown by the marks in the figure, are in good agreement with the numerical results, from which the prediction of numerical results of Q^o from L , Δ , Φ , and Sc is possible.

The comparison of the flow rate of transmitted pure water per unit width of the channel in the case where only one side of the channel is laminated with the RO membrane with those in the case where both sides of the channel are laminated with the RO membrane is shown in Fig. 9. In both cases the existence of the optimum width of the channel at which the flow rate of transmitted pure water becomes maximum is realized. Though the surface area of the membrane in the channel is twice as large as that of

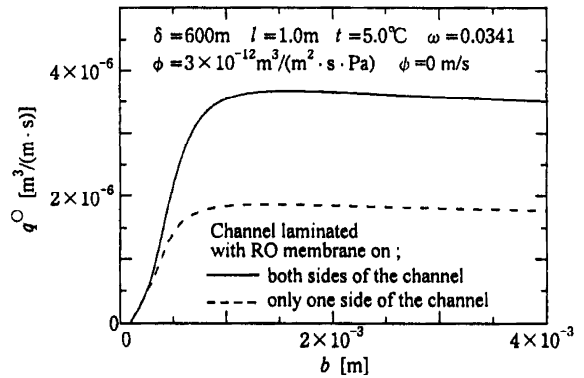


Fig. 9. Comparison of flow rate of transmitted pure water per unit width of channel in the case where only one side of the channel is laminated with the RO membrane with those in the case where both sides of the channel are laminated.

the case where only one side of the channel is laminated with the RO membrane, q^o does not double since the effect of the decrease of driving pressure difference for the water permeation, caused by the rise of the concentration of sea-water in the channel, becomes larger. However, it is possible to make a more compact design for the RO desalination system in comparison with the system in the case where only one side of channel is laminated with the RO membrane.

5. Conclusions

Numerical analyses were performed for the RO desalination system for two cases of the channel configuration. One was the case where only one side of the channel was laminated with the RO membrane, and the other was the case where both sides of the channel were laminated with the RO membrane. In both cases numerical results were obtained for the effects of the width and the axial length of the channel, the submerged depth of the device, the pure water permeability of the membrane, the solute

permeability of the membrane, and the physical properties of seawater or brackish water on the axial variation of velocity, concentration, and pressure in laminar natural convection flow, caused by the concentration difference in the moderately narrow channel. The effect of these parameters on the axial variation of the flow rate of transmitted pure water was also examined. From these results dimensionless expressions were formulated to predict the flow rate of transmitted pure water from those parameters. The existence of the optimum width of the channel at which the flow rate of transmitted pure water becomes maximum is realized.

The field experiments on the desalination system of seawater using static pressure due to the depth of the sea in the case where only one side of the channel was laminated with the RO membrane were carried out in the East China Sea and the Sea of Japan. Experimental results of the flow rate of transmitted pure water were found to be in good agreement with the expression derived from the numerical results, and the applicability and the usefulness of the expression were confirmed.

6. Symbols

b	—	Width of channel, m
C	—	Dimensionless solute concentration of seawater or brackish water defined by Eq. (15)
C^*	—	Dimensionless solute concentration of transmitted fresh water defined by Eq. (15)
$\overline{C^*}$	—	Dimensionless mean solute concentration of transmitted fresh water defined by Eq. (15)
c	—	Solute concentration of seawater or brackish water, kg/m^3
c^*	—	Solute concentration of transmitted fresh water, kg/m^3
$\overline{c^*}$	—	Mean solute concentration of transmitted fresh water, kg/m^3

D	—	Mass diffusivity of solute in water, m^2/s
g	—	Gravitational acceleration, m/s^2
L	—	Dimensionless axial length of channel defined by Eq. (15)
l	—	Axial length of channel, m
P	—	Dimensionless pressure in seawater or brackish water defined by Eq. (15)
p	—	Pressure in seawater or brackish water, Pa
p_v	—	Pressure in transmitted fresh water vessel, Pa
Q	—	Dimensionless induced flow rate in channel defined by Eq. (15)
Q°	—	Dimensionless flow rate of transmitted pure water defined by Eq. (15)
q°	—	Flow rate of transmitted pure water per unit width of channel, $\text{m}^3/(\text{m}\cdot\text{s})$
Sc	—	Schmidt number of seawater or brackish water defined by Eq. (15)
U	—	Dimensionless velocity in X -direction defined by Eq. (15)
u	—	Velocity in x -direction, m/s
V	—	Dimensionless velocity in Y -direction defined by Eq. (15)
v	—	Velocity in y -direction, m/s
X	—	Dimensionless vertical coordinate defined by Eq. (15)
x	—	Vertical coordinate, m
Y	—	Dimensionless horizontal coordinate defined by Eq. (15)
y	—	Horizontal coordinate, m

Greek

Γ	—	Dimensionless concentration coefficient of volumetric expansion defined by Eq. (15)
γ	—	Concentration coefficient of volumetric expansion, m^3/kg
Δ	—	Dimensionless submerged depth of device defined by Eq. (15)

δ	— Submerged depth of device, m
ν	— Kinematics viscosity of seawater or brackish water, m^2/s
π	— Osmotic pressure of seawater or brackish water, Pa
ρ	— Density of seawater or brackish water, kg/m^3
ρ°	— Density of pure water, kg/m^3
ρ^*	— Density of fresh water, kg/m^3
Φ	— Dimensionless pure water permeability of the membrane defined by Eq. (15)
ϕ	— Pure water permeability of the membrane, $\text{m}^3/(\text{m}^2 \cdot \text{s} \cdot \text{Pa})$
Ψ	— Dimensionless solute permeability of the membrane defined by Eq. (15)
ψ	— Solute permeability of membrane, m/s

ω — Solute mass fraction

Subscripts

m	— Mean value
max	— Maximum value
w	— Membrane wall
0	— Ambient seawater or brackish water

References

- [1] B.C. Drude, Desalination, 2 (1967) 325.
- [2] D. Colombo, M. de Gerloni and M. Reali, Desalination, 122 (1999) 171.
- [3] E.F. Miller, Chem. Engineering, 18 (1968) 153.
- [4] M. Reali, M. de Gerloni and A. Sampaolo, Desalination, 109 (1997) 269.
- [5] P. Glueckstern, Desalination, 40 (1982) 143.